Published in final edited form as:
J Mol Med (Berl). 2013 October ; 91(10): 1185–1197. doi:10.1007/s00109-013-1064-7.

Cardiac Glutaminolysis: A Maladaptive Cancer Metabolism Pathway in the Right Ventricle in Pulmonary Hypertension

Lin Piao[†,*], **Yong-Hu Fang**[†,*], **Kishan Parikh**[†], **John J. Ryan**[#], **Peter T. Toth**[†], and **Stephen L. Archer**[†,$]

[†]Section of Cardiology, Department of Medicine, University of Chicago, Chicago, IL, United States

[#]Division of Cardiology, Department of Medicine, University of Utah, Salt Lake City, UT

[$]Department of Medicine, Queen's University, Kingston, Ontario, Canada

Abstract

Rationale—Rapid growth of cancer cells is permitted by metabolic changes, notably increased aerobic glycolysis and increased glutaminolysis. Aerobic glycolysis is also evident in the hypertrophying myocytes in right ventricular hypertrophy (RVH), particularly in association with pulmonary arterial hypertension (PAH). It is unknown whether glutaminolysis occurs in the heart. We hypothesized that glutaminolysis occurs in RVH and assessed the precipitating factors, transcriptional mechanisms and physiological consequences of this metabolic pathway.

Methods and Results—RVH was induced in two models, one with PAH (Monocrotaline-RVH) and the other without PAH (pulmonary artery banding, PAB-RVH). Despite similar RVH, ischemia as determined by reductions in RV VEGFα, coronary blood flow and microvascular density was greater in Monocrotaline-RVH versus PAB-RVH. A 6-fold increase in ^{14}C-glutamine metabolism occurred in Monocrotaline-RVH but not PAB-RVH. In the RV working-heart model, the glutamine antagonist 6-Diazo-5-oxo-L-norleucine (DON) decreased glutaminolysis, caused a reciprocal increase in glucose oxidation and elevated cardiac output. Consistent with increased glutaminolysis in RVH, RV expression of glutamine transporters (SLC1A5 and SLC7A5) and mitochondrial malic enzyme were elevated (Monocrotaline-RVH>PAB-RVH>Control). Capillary rarefaction and glutamine transporter upregulation also occurred in RVH in patients with PAH. cMyc and Max, known to mediate transcriptional upregulation of glutaminolysis, were increased in Monocrotaline-RVH. *In vivo*, DON (0.5 mg/Kg/Da×3 weeks) restored pyruvate dehydrogenase activity, reduced RVH and increased cardiac output (89±8, vs. 55±13 ml/min, $p<0.05$) and treadmill distance (194±71, vs. 36 ±7 m, $p<0.05$) in Monocrotaline-RVH.

Conclusions—Glutaminolysis is induced in the RV in PAH by cMyc-Max, likely as a consequence of RV ischemia. Inhibition of glutaminolysis restores glucose oxidation and has therapeutic benefit *in vivo*.

Keywords

Warburg effect; cMyc; 6-Diazo-5-oxo-L-norleucine (DON); glucose oxidation; WHO Group 1 pulmonary hypertension (PAH); anapleurosis; congenital heart disease

Address for correspondence: Stephen L. Archer MD. FRCP(C), FAHA, FACC, Professor and Head, Department of Medicine, Queen's University, Etherington Hall, Room 3041, 94 Stuart St., Kingston, Ontario, Canada, K7L 3N6, stephen.archer@queensu.ca, Telephone: 613 533-6327, Fax: 613 533-6695.
[*]These authors contributed equally to this work

Disclosures No conflicts to disclose.

Introduction

A shift in glucose metabolism from glucose oxidation (GO) to aerobic glycolysis, the so-called Warburg effect[1], and induction of glutaminolysis[2] are hallmarks of cancer metabolism. These two metabolic abnormalities often occur in tandem, perhaps because they can both be upregulated by activation of proto-oncogene cMyc[2, 3]. These metabolic pathways promote rapid cell growth and proliferation and offer potential therapeutic targets for tumor regression[3, 4]. Intriguingly, aerobic glycolysis occurs in pulmonary vascular cells[5, 6] and hypertrophied right ventricular myocytes[7] in pulmonary arterial hypertension (PAH). This caused us to postulate that glutaminolysis might also be induced in the heart under conditions of right ventricular hypertrophy (RVH).

Although GO and fatty acid oxidation (FAO) are the classical metabolic pathways for cardiac adenosine triphosphate (ATP) generation in adult hearts[8], metabolic plasticity occurs in the heart during development and with acquired pathologies, such as hypertrophy and ischemia. In PAH-associated RVH a maladaptive metabolic switch to aerobic glycolysis[7] is mediated by increased pyruvate dehydrogenase kinase (PDK4), expression and activity, resulting in inhibition of pyruvate dehydrogenase (PDH)[9]. ATP production by this less efficient process is supported by increased glucose influx, mediated via upregulated expression of glucose transporter 1 (Glut1). This energetic response to pressure overload supports myocyte growth at the price of generation of increased lactic acid production, bioenergetic impairment, and impaired RV function. PDK inhibitors, such as dichloroacetate, restore PDH activity and GO and improve RV function in experimental models of RVH[7, 10].

The role of glutaminolysis in the heart is unknown. However, in cancer glutamine can support cell metabolism by oxidation to CO_2 yielding ATP[3]. Glutamine can also be hydrolysed to glutamate and subsequently converted to α-ketoglutarate (α-KG) in the mitochondria. α-KG can enter Krebs' cycle and replenish the metabolic intermediates thereby supporting the biosynthetic demands for nicotinamide adenine dinucleotide phosphate (NADPH) and fatty acids during rapid cell growth. This replenishment of the metabolic intermediates is called *anapleurosis*. Glutaminolysis may also support cell growth by increasing nitrogen anabolism[3].

There are similarities between aerobic glycolysis and glutaminolysis. For example, lactate generation is increased in glutaminolysis (in this case via malic enzyme, Me)[11]. In addition, the high glutamine influx required by glutaminolysis requires upregulation of the glutamine transporters, SLC1A5 and SLC7A5[3], analogous to the upregulation of the Glut1 transporter in aerobic glycolysis[7, 10].

Changes in glutamine and glutamate uptake have been noted in chronic ischemic heart disease[12, 13]. Based on studies using positron emission tomography, Knapp *et al.* suggested glutamate utilization may be involved in metabolic adaptation in ischemic myocardium in patients with coronary artery disease[14]. Additional circumstantial evidence of cardiac glutaminolysis includes the observation of elevated serum glutamine levels during acute myocardial ischemia[15] and the activation of cMyc in left ventricular hypertrophy and ischemia[16]. However, to our knowledge glutaminolysis has never been directly measured in the heart nor are its consequences known.

We hypothesized that RV ischemia and cMyc activation in PAH-associated RVH initiate cardiac glutaminolysis. We speculated that glutaminolysis might contribute to the increased myocyte growth in RVH. We studied this in two rodent RVH models, one associated with PAH (Monocrotaline-RVH) and another in which RVH is induced by pulmonary artery banding (PAB). Despite identical severity of hypertrophy, Monocrotaline-RVH is

maladaptive with more severe ischemia, autonomic remodeling and RV dysfunction as compared to PAB-RVH[17]. Indeed, in Monocrotaline-RVH abnormalities of metabolic and adrenergic signaling extend to the left ventricle. The microvascular rarefaction in certain forms of RVH, such as Monocrotaline-RVH, may be conducive to glutaminolysis, since it could promote ischemia. Because PAB-RVH has much less capillary rarefaction, it is an excellent comparator model[18]. A specific glutaminolysis inhibitor, 6-Diazo-5-oxo-L-norleucine (DON), was used to determine the physiologic consequences of increased cardiac glutaminolysis. Results in rodent RVH are also tested in patients with PAH and RVH.

In this study we provide an initial description of right ventricular glutaminolysis, propose a mechanism for its induction (ischemia-induced activation of cMyc) and demonstrate a novel reciprocal relationship between glutaminolysis and GO. Glutaminolysis is maladaptive and inhibition of glutaminolysis has therapeutic promise in RVH.

Methods and Materials

All authors have read and agreed to the manuscript as written.

Experimental protocols

The University of Chicago Institutional Animal Care and Use Committee approved all rodent protocols. The institutional review board approved the use of autopsied human tissues for research. The demographics of the control, idiopathic PAH and scleroderma PAH patients are in the Online Supplement.

RVH models

RVH models were created, as previously described, in male Sprague-Dawley rats (260-280g)[7]: (1) PAB-RVH was induced by surgical placement of a 1.3mm PA band. A median sternotomy was performed and the PA was dissected free from the aorta and left atrium. A silk suture was placed around the PA and a loose knot formed. A 16-gauge needle was inserted through the knot, parallel to the PA. The suture was tied tightly and the needle was withdrawn, creating a stenosis equal to the needle's diameter (~1.6 mm). (2) Monocrotaline-RVH was induced by a single subcutaneous injection of monocrotaline (60mg/Kg, SC, Sigma, St. Louis, MO). Endpoints were measured after 4-weeks. In additional cohorts, 6-Diazo-5-oxo-L-norleucine (DON, 0.5 mg/Kg/Da×3 weeks, Sigma) was injected intraperitoneally, beginning 1-week after monocrotaline injection.

Echocardiography

A Vevo 2100 (Visual Sonics, Toronto, Ontario, Canada) was used to assess pulmonary artery acceleration time (PAAT), right ventricular free wall (RVFW), stroke volume (SV), tricuspid annular plane systolic excursion (TAPSE) and RV function, as previously described[10]. Transthoracic echocardiogram was performed on lightly anesthetized but spontaneously breathing rats (isoflurane 2.0% in medical gas)[7, 10]. RVFW diastolic thickness was assessed by two-dimensional and M-mode echocardiography using right parasternal long-axis imaging views with the ultrasonic beam positioned perpendicularly to the wall in the proximal part of the mid-third of the RV.

TAPSE was measured as a marker of RV function. TAPSE was measured by placing the M-mode cursor through the lateral portion of the tricuspid annular plane in the apical four-chamber view and measuring systolic excursion.

Treadmill distance

Exercise capacity was tested by measuring the maximal distance run on a motorized treadmill (Simplex II Instrument; Columbus Instruments, Columbus, OH), as described[10]. The initial treadmill speed was 10 m/min and increased 5 m/min every 5 min for 30 minutes or until the rat fatigued. The treadmill distances in control versus the RVH model was measured 4-weeks after monocrotaline injection.

RVH

RVH was measured postmortem as the ratio of RV/(LV+septum) weight.

Coronary flow measurement

In RV Langendorff, the perfusate was collected from the coronary sinus. Total coronary flow was corrected for collection time and body weight.

Thermodilution cardiac output

After anesthesia, the jugular vein and carotid artery were cannulated by the cut down technique. A thermistor probe catheter (Physitemp Instruments, Inc., Clifton, NJ) was inserted into the aorta via the carotid artery. A catheter was inserted into the right atrium via the jugular vein. 0.3ml ice-cold saline was then quickly injected into the right atrium and a thermodilution curve (temperature vs. time) was recorded. PowerLab (ADInstruments Inc, Colorado Springs, CO) was used for data acquisition. CO was then determined by calculating the area under the temperature curve.

Measurement of ^{14}C-glutamine or ^{14}C-glucose metabolism in the RV working heart model

The RV working heart model was used to simultaneously measure metabolism and cardiac function, as previously described[7]. The heart was rapidly excised and subsequently mounted on an aortic perfusion cannula for about 10 minutes. The pulmonary veins, main PA and superior vena cava were isolated and cannulated. The inferior vena cava was isolated and ligated. To initiate flow to the RV and left ventricle (LV), perfusate was delivered to the superior vena cava and left atria cannulae, respectively, at constant preload (45 mmHg and 115 mmHg, respectively). Hearts worked against a 80 mm Hg aortic afterload, and a 45 mm Hg PA afterload. Cardiac output (CO) and stroke work (SW) were measured with a Millar pressure-volume catheter (Millar, Houston, TX). The signals were recorded using MPVS Ultra Single Segment System (Millar, Houston, TX) and analyzed using Chart V 5.5.6 (ADInstruments Inc, Colorado Springs, CO).

Glutaminolysis and glucose oxidation were measured by perfusing hearts with Krebs-Henseleit buffer containing 2 mM [^{14}C]glutamine+5mM glucose or 11 mM [^{14}C] glucose, 0.5 mM lactate, 1.2 mM palmitate, 3% albumin, and 100 U/ml insulin. The dose of 2 mM glutamine was selected based on concentrations commonly used in the culture medium for cardiac myocytes[19, 20] and in working heart perfusate solutions [21, 22]. The effects of 6-Diazo-5-oxo-L-norleucine (DON) on glutaminolysis, glucose oxidation and cardiac function were evaluated by quantitative collection of $^{14}CO_2$ at 10 minute intervals after adding 5 μM or 10μM DON to the perfusate.

A pressure–volume signal was continuously recorded at sampling rate of 1000/s using an MPVS-300 (ADInstruments Inc, Colorado Springs, CO) coupled to a PowerLab8/30 converter (ADInstruments). CO and stroke volume were computed using pressure–volume analysis software (Labchart7.2; ADInstruments).

Cytosolic glutamine, malate and lactate level were measured following the manufacturer's instructions (Abcam, Cambridge, MA).

qRT-PCR

RNA extraction and quantitative RT-PCR (qRT-PCR) was performed per the manufacturer's protocol (Applied Biosystems, Foster City, CA). mRNA levels of cMyc, its partner Max, HIF-1α, vascular endothelial growth factor α (VEGFα), glucose transporter 1 (Glut1), hexokinase 1 (HK1), HK2, glutamine transporter SLC7A5 and SLC1A5, glutaminase (GLS), mitochondrial and cytosolic malic enzyme (Me1 and Me2) were assessed by a ABI PRISM 7900HT PCR system (Applied Biosystems). mRNA expression was normalized to 18S mRNA.

Immunoblot

Nuclear proteins from RV tissues were isolated following the manufacturer's instructions (Thermo Scientific, Rockford, IL). Western blots were performed using standard procedures[7].

Immunofluorescence

Frozen sections were fixed in methanol, blocked with albumin (Sigma, St. Louis, MO), and incubated with primary antibodies for 1 hour at 25°C (mouse monoclonal anti-dystrophin, 1:400 dilution, rabbit polyclonal anti-cMyc and anti-SLC1A5 1:500 dilution, Abcam, Cambridge, MA). Immunostaining was performed using standard procedures.

Capillary staining

RV tissue microarray samples from patients with idiopathic PAH, scleroderma-associated PAH and the patients without PAH (control) (Supplemental Table for clinical data) were stained for the endothelial marker CD31 and smooth muscle actin. RV sections from both rodent RVH models and control were stained with another endothelial marker, tomato lectin. Images were obtained with a Zeiss Axio Observer Z1 inverted microscope and capillary densities were analyzed by using ImageJ (NIH, Bethesda, MD).

Statistics and sample size

Values were expressed as mean±SEM. Comparisons between groups used an ANOVA or unpaired Student's *t*-test, as appropriate. Post hoc testing used a Bonferroni's correction. $P<0.05$ was considered statistically significant.

Results

RV/LV+septum ratio was similarly increased in PAB-RVH (0.51±0.02) and Monocrotaline-RVH (0.54±0.03) vs. control (0.26±0.01) ($p<0.01$).

RV working heart and metabolism

In the presence of glutamine in the perfusate[22], low rates of glutaminolysis were noted in control and PAB-RVH groups. Direct measurement of $[^{14}C]CO_2$-derived from $[^{14}C]$glutamine, revealed a ~6-fold increase in glutaminolysis in Monocrotaline-RVH versus control (2.83±0.57 vs. 0.48±0.12 $\mu M \bullet g^{-1} \bullet min^{-1}$, Fig 1A). Acute administration of DON (5μM) significantly reduced glutaminolysis in Monocrotaline-RVH (0.22±0.07 $\mu M \bullet g^{-1} \bullet min^{-1}$, Fig 1A) without altering rates in control hearts. Although there was no increase in glutaminolysis in PAB-RVH hearts compared to control hearts, DON did significantly lower the rate of glutaminolysis in PAB-RVH (0.19±0.01 vs. 0.44±0.04 $\mu M \bullet g^{-1} \bullet min^{-1}$, Fig 1A).

In the absence of glutamine (with glucose as the only substrate), GO, measured as [^{14}C] CO_2 derived from [^{14}C] glucose, was markedly reduced in RVH (0.03±0.01 vs. 0.19±0.03 $\mu M \bullet g^{-1} \bullet min^{-1}$, Fig 1B), as previously described[7]. Addition of glutamine reduced rates of GO in control hearts. Conversely, in the presence of glutamine, DON significantly increased GO in control and in both RVH models (control: 0.09±0.01 vs. 0.04±0.01; PAB: 0.15±0.03 vs. 0.07±0.01; Monocrotaline: 0.08±0.01 vs. 0.03±0.01 $\mu M \bullet g^{-1} \bullet min^{-1}$). Consistent with the increased glutaminolysis being greatest in Monocrotaline-RVH, DON increased CO and SW in Monocrotaline-RVH without significantly altering hemodynamics in PAB-RVH (CO: 193±22 vs. 111±19 ml/min; SW: 27±2 vs. 15±3 mmHg•ml, Fig 1C-D). DON did cause an unexplained increase in CO in control hearts but did not change SW. Together, these findings indicate that there is minimal glutaminolysis in control hearts and that glutaminolysis is markedly elevated in Monocrotaline-RVH. Glutaminolysis appears to be maladaptive since inhibiting glutaminolysis increases CO and SW in Monocrotaline-RVH.

Increased expression of cMyc-Max in RVH

In Monocrotaline-RVH there was a biventricular increase in mRNA expression of cMyc and Max (Fig 2A). In PAB-RVH, Max was not increased (Fig 2A). Increased cMyc was also seen in immunohistochemistry staining of the RV (Fig 2B). The results from immunostaining and an immunoblot performed on the nuclear extracts from RV myocytes confirmed that the cMyc was activated, evident as increased nuclear localization (Fig 2B-C). The success of the nuclear fractionation was confirmed by the presence of the nuclear protein topoisomerase 1 in the nuclear fraction (Fig 2C).

Increased expression of glutamine transporters in RVH

In Monocrotaline-RVH there was a biventricular increase in mRNA expression of glutamine transporters SLC1A5 and SLC7A5 (Fig 3A-B, Supplemental Fig 1A). In PAB-RVH, only SLC7A5 expression was increased and only in the RV (Fig 3A). Glutaminase expression was unaltered by either form of RVH (Supplemental Fig 1B). Interestingly, cytosolic malic enzyme (Me1) was reduced in Monocrotaline-RVH and elevated in PAB-RVH (Fig 3B) whereas mitochondrial malic enzyme (Me2) was increased only in Monocrotaline-RVH. Protein expression of SLC1A5 was significantly increased in Monocrotaline-RVH (Fig 3C). Consistent with the pattern of change in expression of glutamine transporter genes and Me2, the RV tissue levels of glutamine, malate and lactate increased more in Monocrotaline-RVH versus PAB-RVH (Fig 4A). Moreover, plasma glutamine and malate levels also increased significantly in Monocrotaline-RVH but not PAB-RVH (Fig 4B).

Glycolytic genes, Glut1 and Hexokinase1 (HK1) were increased in both RVH models, whereas HK2 was only increased in Monocrotaline-RVH (Supplemental Fig 1C). HIF-1α was also only increased in Monocrotaline-RVH but not PAB-RVH (Supplemental Fig 1D). Protein expression of HIF-1∝ in the nuclei of RV myocytes was present in Monocrotaline-RVH, although this finding could not be reproduced in all experiments (data not shown).

Microvascular rarefaction

Reduction in coronary flow and capillary rarefaction was noted in both models but was most severe in Monocrotaline-RVH (Fig 5A-C). Consistent with this, biventricular reduction in VEGFα mRNA was restricted to Monocrotaline-RVH (Fig 5D). Capillary rarefaction also occurred in PAH patients, particularly those with scleroderma PAH (Fig 5E&F, see demographics in Supplemental Table 1).

In vivo therapy with chronic DON

Since glutaminolysis was primarily evident in Monocrotaline-RVH we focused *in vivo* studies of chronic DON on the Monocrotaline rat. DON reduced RVH in Monocrotaline rats, evidenced by the reduced RV/LV+Septum ratio (0.43±0.04 vs. 0.60±0.02) and RVFW (0.53±0.04 vs. 1.00±0.13 mm, Fig 6A&B). DON increased CO and treadmill distance in Monocrotaline rats (CO: 89±8 vs. 55±13 ml/min; treadmill distance: 194±70 vs. 36±7 m, Fig 6D&E). DON reduced body weight in control but not in Monocrotaline rats (control: 412±10 vs. 528±12 g; Monocrotaline: 430±19 vs. 365±28 g, Supplemental Fig 2A). DON tended to reduce RVSP (51.2±6.0 to 39.3±2.4 mmHg; p=0.08, Supplemental Fig 2C) and in a study with increased DON dosage, significantly increased PAAT, but only when given in high doses which had systemic toxicity in Monocrotaline-induced RVH (Supplemental Fig 3C). This suggests that DON not only improves cardiac function but also may have beneficial effects on the pulmonary vasculature. DON did significantly increase TAPSE in Monocrotaline rats (control: 1.12±0.16 vs. 1.81±0.16; Monocrotaline: 0.97±0.06 vs. 0.59±0.11 mm, Figure 6C). These findings indicate that inhibiting glutaminolysis is beneficial and suggest that DON's beneficial effects on CO and treadmill time are related primarily to effects on the RV. However, potential effects of DON on the pulmonary vasculature require further study.

DON therapy normalized RV myocyte levels of glutamine and glutamate (Fig 6F). DON also reduced the expression of key mediators of glutaminolysis (cMyc, SLC1A5, SLC7A5, Me2 mRNA, Fig 7A-C) and glycolytic genes (Glut1 and HK1, Supplemental Fig 2D&E). Consistent with the acute ability of DON to increase GO in RVH (Fig 1B), chronic DON therapy restored PDH activity in Monocrotaline-RVH (Fig 7D). This suggests that the inhibition of glutaminolysis may exert its benefits by enhancing GO. DON therapy reduced the mRNA expression of VEGFα (Supplemental Fig 2F), suggesting DON therapy is not able to correct ischemia in RVH.

In PAH patients, immunostaining results confirmed that SLC1A5 proteins were increased in the RV, particularly in the RV myocytes plasma membrane (Fig 8A).

Discussion

The current study reveals that cardiac glutaminolysis is induced in the maladaptive RVH that accompanies Monocrotaline-induced PAH. DON-sensitive glutaminolysis is increased ~6-fold in Monocrotaline-RVH with a small DON-sensitive rate of glutaminolysis being evident in PAB-RVH. This difference in glutaminolysis between models likely reflects the greater ischemia seen in Monocrotaline-RVH (evident in greater reduction in VEGFα expression, RV capillary density and coronary blood flow). Monocrotaline-RVH's greater ischemic burden is associated with activation of cMyc-Max signaling, evident by the upregulation of glutamine transporters. Although cMyc is upregulated in PAB-RVH, its binding partner Max is only increased in Monocrotaline-RVH (Fig 2A). Both capillary rarefaction and increased glutamine transporter expression were also seen in the RV's of patients with PAH-RVH (Fig 5E&F). Importantly, the inhibition of glutaminolysis by acute or chronic DON treatment in Monocrotaline-RVH improves GO and improves RV function (Fig 1&7), suggesting a new therapeutic strategy on treating RVH.

We demonstrate that the inhibition of glutaminolysis improves GO. This is reminiscent of the reciprocal relationship between GO and FAO (the Randle cycle), which we have previously exploited therapeutically in RVH[10]. In the case of the Randle cycle, it is FAO metabolites (such as citrate) that inhibit GO whilst FAO inhibitors, such as trimetazidine, restore GO in RVH[10]. We speculate that glutaminolysis-derived products similarly suppress GO. DON rapidly (<30 minutes) inhibits glutaminolysis and restores GO (Fig 1).

Although the switch back to GO in the working heart model is too rapid to be transcriptionally mediated, there are additional transcriptionally-mediated interactions that may be relevant to the ability of chronic DON therapy to restore PDH activity (Fig 7). Kaadige et al. reported that glutamine-dependent mitochondrial anapleurosis dictates glucose uptake and aerobic glycolysis by blocking MondoA:Mlx-dependent transcriptional activation of thioredoxin-interacting protein[23]. Inhibition of glutaminolysis with aminooxyacetate, which prevents conversion of glutamate to α-KG, restricts glucose uptake in pancreatic cancer cell lines[23]. They proposed that this mechanism coordinates glutamine and glucose utilization serving as a "metabolic checkpoint that restricts cell growth when subthreshold levels of these essential nutrients are present" [23].

We have previously found that both PAB and Monocrotaline-RVH have a metabolic switch from GO to glycolysis[7]. Interestingly, PAB, a model of adaptive RVH[17, 18] manifests several differences in glutamine metabolism as compared with Monocrotaline-RVH, a maladaptive model. Unlike in Monocrotaline-RVH, SLC1A5, Max and Me2 mRNA are not increased in PAB-RVH. Consistent with this, glutaminolysis is quantitatively much less in PAB-RVH. Indeed, the only evidence of a slight increase in glutaminolysis in PAB-RVH is the finding that DON does lower glutaminolysis levels significantly (albeit by a small absolute amount) (Fig 1).

The metabolic roles of Me1 and Me2 have not been fully resolved. Malate is an important Krebs' cycle intermediate and can be exported from the mitochondria to the cytosol. Both pyruvate carboxykinase and cytosolic $NADP^+$-dependent Me1 support the pyruvate cycling, which is a necessary step for glucose-stimulated insulin secretion[24]. The increased Me1 in PAB-RVH may be helpful in pyruvate cycling so that more pyruvate influxes into the mitochondria, thereby assisting in ATP creation through Krebs' cycle. Conversely, in Monocrotaline-RVH the reduced Me1 decreases the ability of pyruvate to influx into the mitochondria. Glutaminolysis-derived Me2 can also provide an alternative source of pyruvate when pyruvate flux from glycolysis is limited[25]. In the current study chronic DON therapy reduced expression of Me2 but not Me1 (Fig 7C). In pancreatic beta cells, Me1 knockdown decreases flux of pyruvate derived from both glycolysis and glutamine-related pools through pyruvate carboxylase[24]. In contrast, Me2 knockdown affects only the flux of the pyruvate that derives from glutamate metabolism[24]. Further study will be required to determine which malate enzyme isoform is most relevant for cardiac glutaminolysis. The marked increase in expression of Me2 in Monocrotaline-RVH, which reverses with DON (Fig 3), argues for an important role for this isoform in the metabolic phenotype of RVH (Figure 8B).

The plasma and RV tissue levels of glutamine are increased in RVH (Figures 4 and 6F). The markedly increased expression of SLC1A5 and SLC7A5 in the RV in RVH suggest an increased glutamine uptake (Fig 3). This is consistent with the increased glutamine level in the RV tissues. Meanwhile, as shown in Fig 4 and Fig 6, the levels of glutamate, malate and lactate were all increased in RV tissues in the Monocrotaline model, suggesting increased glutaminolysis in RVH.

It is well-known that cMyc is the key regulator for glutamine metabolism[26]. In the current study it is apparent not only that cMyc activation is associated with an increase in RV glutamine metabolism, but also that chronic administration of DON reduced cMyc and glutamine transporters' expression in the RV in rats with RVH. This suggests that there is a bidirectional positive feedback relationship between cMyc and glutaminolysis. This observation is consistent with that seen in human choriocarcinoma cells in which DON significantly reduced cMyc mRNA expression[27].

In cancer, cMyc orchestrates transcriptional upregulation of glutaminolysis[26, 28]. In cancer cells, cMyc cooperates with HIF-1α by binding to E-boxes of glycolytic genes, thereby promoting glycolysis. cMyc is also essential for glutaminolysis by regulating SLC1A5 and glutaminase[2]. cMyc is essential for vasculogenesis and angiogenesis and is required for the expression of VEGFα[29]. Activation of cMyc in the heart has been reported to occur as a result of ischemia in LVH[16]. It is likely that cMyc activation in RVH reflects capillary rarefaction and RV ischemia (Fig 5). The relationship between ischemia/hypoxia, VEGFα and cMyc in the heart requires further investigation.

The purpose of glutaminolysis in RVH remains uncertain. Extrapolation from cancer metabolism would suggest that glutaminolysis supports rapid cell growth (myocyte hypertrophy) in RVH. The consequences of RV glutaminolysis is largely negative, evident from the fact that inhibition of glutaminolysis with DON in Monocrotaline-RVH restores GO and improves RV function *ex vivo* (Fig 1), while regressing RVH and increasing exercise capacity *in vivo* (Fig 6).

The importance of glutaminolysis would be missed if one studied only normal hearts. A recent study by Lauzier et al using the working heart preparation found that overall glutamine had little effect on the contractile function. We show the pathway is only induced in RVH. Thus, consistent with Lauzier's findings[30] we conclude there is little glutaminolysis under control condition (Fig 1). However in RVH, the increased glutaminolysis impairs cardiac output and shortens treadmill distance. By reducing glutaminolysis with chronic DON therapy, RVH was reduced and cardiac output and treadmill capacity were improved in RVH.

Limitations

PAB is considered to have less ischemia inducing potential than Monocrotaline because of the relative paucity of microvascular disease in this model. However, PAB may cause a supply-demand mismatch in perfusion that could evoke modest ischemia. The observation that cMyc expression is increased and capillary density is decreased in the PAB-RV, whilst glutaminolysis remains low raises questions as to the relatedness of these observations in PAB-RVH. However, cMyc's obligatory binding partner, Max is not elevated in PAB (Fig 2A), which may reduce cMyc/Max signaling. In addition, the reduction in capillary density in PAB is significantly less than in Monocrotaline-RVH. These observations suggest less severe ischemia and perhaps milder activation of glutaminolysis in PAB-RVH compared to Monocrotaline-RVH. The finding that DON does reduce glutaminolysis (Fig 1A) and increase glucose oxidation (Fig 1B) in PAB-RVH suggests mild induction of glutaminolysis in this condition.

There are unknown off-target effects of DON, which might complicate the interpretation of our findings. However, the careful measurement of glutaminolysis does verify that DON did indeed inhibit glutaminolysis in our studies. DON has dose-limiting neurotoxicity and gastrointestinal toxicity[26]. Consistent with this a higher DON dose (1 mg/Kg/Da×10 days) regressed Monocrotaline-RVH and pulmonary vascular disease but caused severe weight loss and weakness (Supplemental Fig 3). Future studies will need to explore other potential glutaminolysis inhibitors that may have a greater therapeutic window.

In Monocrotaline-RVH, abnormalities in expression of VEGFα, Glut1, SLC7A5, Me2, cMyc and Max extended to the LV (Fig 2-3 & Supplemental Fig 1). Further study is required to definitively establish whether glutaminolysis also occurs in the LV of maladaptive RVH. However, the observation that the LV is involved in a shift to glutaminolysis in Monocrotaline-induced PAH is not entirely unexpected. We recently found that adrenergic remodeling occurs in the LV in this model, albeit to a lesser extent

than in the RV[17]. While we did not prove that the increase in SLC7A5 and cMyc resulted for microvascular rarefaction in the LV, this interpretation is supported by the reduced expression of VEGFα in the LV (Fig 5D).

In the current study, we choose Monocrotaline-RVH as a maladaptive model (heart failure model) combined with PAH and RVH. As a comparison, PAB-RVH does not develop lung disease, PAH or heart failure after PAB surgery[32]. Glutamine metabolism could also be accessed in another RVH model such as chronic hypoxia + SU-5416 (a VEGF receptor inhibitor).

In the RV working heart model we used 2 mM glutamine in the perfusate. While this is likely higher than that seen *in vivo* (Figure 4B), it is a commonly used dose in the literature and had no acute adverse effect on cardiac function (Supplemental Fig 4).

Although the glutaminolysis pathway is an intriguing target for new PAH therapeutics it must be acknowledged that DON was abandoned as a cancer therapeutic because of toxicity. There are other drugs that have effects on glutaminolysis. For example, phenylbutyrate (also called ammonaps) is an FDA approved agent for the treatment of hyperammonemia in congenital urea cycle disorders and has shown a significant effect on depleting plasma glutamine[33]. *In vitro* treatment of lung cancer cells with L-g-glutamyl-p-nitroanilide (GPNA; an inhibitor of SLC1A5) decreased cancer cell growth and viability by inhibiting SLC1A5 and lowering glutamine levels[34]. Further studies of these and other modulators of glutaminolysis are indicated in PAH-RVH models. Direct cMyc inhibition, using small molecule inhibitors such as 10058-F4[31], may be an alternative means of reducing glutaminolysis.

HIF-1α mRNA levels were increased in Monocrotaline-RVH (Supplemental Figure 1D). However there was nuclear translocation of HIF-1α, consistent with its activation, in the limited number of Monocrotaline-RVH specimens assessed (data not shown).

Conclusions

To our knowledge, this is the first demonstration of cardiac glutaminolysis. The metabolic parallels between RVH and cancer are now expanded to include glutaminolysis, as well as aerobic glycolysis (Fig 8B). Inhibition of glutaminolysis has potential as a metabolic therapy targeting the right ventricle.

Supplementary Material

Refer to Web version on PubMed Central for supplementary material.

Acknowledgments

Dr. Archer is supported by NIH-RO1-HL071115 and 1RC1HL099462-01 and the American Heart Association. The authors thank Dr. E. Kenneth Weir for his help in critiquing this manuscript.

References

1. Kim JW, Dang CV. Cancer’s molecular sweet tooth and the Warburg effect. Cancer Res. 2006; 66:8927–8930. [PubMed: 16982728]
2. Dang CV. Therapeutic targeting of Myc-reprogrammed cancer cell metabolism. Cold Spring Harb Symp Quant Biol. 2011; 76:369–374. [PubMed: 21960526]
3. Dang CV. Glutaminolysis: supplying carbon or nitrogen or both for cancer cells? Cell cycle. 2010; 9:3884–3886. [PubMed: 20948290]

4. Bonnet S, Archer SL, Allalunis-Turner J, Haromy A, Beaulieu C, Thompson R, Lee CT, Lopaschuk GD, Puttagunta L, Harry G, et al. A mitochondria-K+ channel axis is suppressed in cancer and its normalization promotes apoptosis and inhibits cancer growth. Cancer Cell. 2007; 11:37–51. [PubMed: 17222789]
5. Xu W, Koeck T, Lara AR, Neumann D, DiFilippo FP, Koo M, Janocha AJ, Masri FA, Arroliga AC, Jennings C, et al. Alterations of cellular bioenergetics in pulmonary artery endothelial cells. Proc Natl Acad Sci U S A. 2007; 104:1342–1347. [PubMed: 17227868]
6. Marsboom G, Wietholt C, Haney CR, Toth PT, Ryan JJ, Morrow E, Thenappan T, Bache-Wiig P, Piao L, Paul J, et al. Lung (1)(8)F-fluorodeoxyglucose positron emission tomography for diagnosis and monitoring of pulmonary arterial hypertension. Am J Respir Crit Care Med. 2012; 185:670–679. [PubMed: 22246173]
7. Piao L, Fang YH, Cadete VJ, Wietholt C, Urboniene D, Toth PT, Marsboom G, Zhang HJ, Haber I, Rehman J, et al. The inhibition of pyruvate dehydrogenase kinase improves impaired cardiac function and electrical remodeling in two models of right ventricular hypertrophy: resuscitating the hibernating right ventricle. J Mol Med. 2010; 88:47–60. [PubMed: 19949938]
8. Stanley WC, Lopaschuk GD, Hall JL, McCormack JG. Regulation of myocardial carbohydrate metabolism under normal and ischaemic conditions. Potential for pharmacological interventions. Cardiovasc Res. 1997; 33:243–257. [PubMed: 9074687]
9. Marsboom G, Toth PT, Ryan JJ, Hong Z, Wu X, Fang YH, Thenappan T, Piao L, Zhang HJ, Pogoriler J, et al. Dynamin-related protein 1-mediated mitochondrial mitotic fission permits hyperproliferation of vascular smooth muscle cells and offers a novel therapeutic target in pulmonary hypertension. Circ Res. 2012; 110:1484–1497. [PubMed: 22511751]
10. Fang YH, Piao L, Hong Z, Toth PT, Marsboom G, Bache-Wiig P, Rehman J, Archer SL. Therapeutic inhibition of fatty acid oxidation in right ventricular hypertrophy: exploiting Randle's cycle. J Mol Med (Berl). 2012; 90:31–43. [PubMed: 21874543]
11. DeBerardinis RJ, Mancuso A, Daikhin E, Nissim I, Yudkoff M, Wehrli S, Thompson CB. Beyond aerobic glycolysis: transformed cells can engage in glutamine metabolism that exceeds the requirement for protein and nucleotide synthesis. Proc Natl Acad Sci U S A. 2007; 104:19345–19350. [PubMed: 18032601]
12. Bing RJ, Siegel A, Ungar I, Gilbert M. Metabolism of the human heart. II. Studies on fat, ketone and amino acid metabolism. Am J Med. 1954; 16:504–515. [PubMed: 13148192]
13. Mudge GH Jr. Mills RM Jr. Taegtmeyer H, Gorlin R, Lesch M. Alterations of myocardial amino acid metabolism in chronic ischemic heart disease. J Clin Invest. 1976; 58:1185–1192. [PubMed: 993339]
14. Knapp WH, Helus F, Ostertag H, Tillmanns H, Kubler W. Uptake and turnover of L-(13N)-glutamate in the normal human heart and in patients with coronary artery disease. Eur J Nucl Med. 1982; 7:211–215. [PubMed: 6124422]
15. Bodi V, Sanchis J, Morales JM, Marrachelli VG, Nunez J, Forteza MJ, Chaustre F, Gomez C, Mainar L, Minana G, et al. Metabolomic profile of human myocardial ischemia by nuclear magnetic resonance spectroscopy of peripheral blood serum: a translational study based on transient coronary occlusion models. J Am Coll Cardiol. 2012; 59:1629–1641. [PubMed: 22538333]
16. Ahuja P, Zhao P, Angelis E, Ruan H, Korge P, Olson A, Wang Y, Jin ES, Jeffrey FM, Portman M, Maclellan WR. Myc controls transcriptional regulation of cardiac metabolism and mitochondrial biogenesis in response to pathological stress in mice. J Clin Invest. 2010; 120:1494–1505. [PubMed: 20364083]
17. Piao L, Fang YH, Parikh KS, Ryan JJ, D'Souza KM, Theccanat T, Toth PT, Pogoriler J, Paul J, Blaxall BC, et al. GRK2-Mediated Inhibition of Adrenergic and Dopaminergic Signaling in Right Ventricular Hypertrophy: Therapeutic Implications in Pulmonary Hypertension. Circulation. 2012; 126:2859–2869. [PubMed: 23124027]
18. Bogaard HJ, Natarajan R, Henderson SC, Long CS, Kraskauskas D, Smithson L, Ockaili R, McCord JM, Voelkel NF. Chronic pulmonary artery pressure elevation is insufficient to explain right heart failure. Circulation. 2009; 120:1951–1960. [PubMed: 19884466]

19. Sartoretto JL, Kalwa H, Shiroto T, Sartoretto SM, Pluth MD, Lippard SJ, Michel T. Role of Ca2+ in the control of H2O2-modulated phosphorylation pathways leading to eNOS activation in cardiac myocytes. PLoS One. 2012; 7:e44627. [PubMed: 22970272]
20. Mohl MC, Iismaa SE, Xiao XH, Friedrich O, Wagner S, Nikolova-Krstevski V, Wu J, Yu ZY, Feneley M, Fatkin D, et al. Regulation of murine cardiac contractility by activation of alpha(1A)-adrenergic receptor-operated Ca(2+) entry. Cardiovasc Res. 2011; 91:310–319. [PubMed: 21546445]
21. Cohen DM, Guthrie PH, Gao X, Sakai R, Taegtmeyer H. Glutamine cycling in isolated working rat heart. Am J Physiol Endocrinol Metab. 2003; 285:E1312–1316. [PubMed: 12944323]
22. Rennie MJ, Khogali SE, Low SY, McDowell HE, Hundal HS, Ahmed A, Taylor PM. Amino acid transport in heart and skeletal muscle and the functional consequences. Biochem Soc Trans. 1996; 24:869–873. [PubMed: 8878864]
23. Kaadige MR, Looper RE, Kamalanaadhan S, Ayer DE. Glutamine-dependent anapleurosis dictates glucose uptake and cell growth by regulating MondoA transcriptional activity. Proceedings of the National Academy of Sciences of the United States of America. 2009; 106:14878–14883. [PubMed: 19706488]
24. Pongratz RL, Kibbey RG, Shulman GI, Cline GW. Cytosolic and mitochondrial malic enzyme isoforms differentially control insulin secretion. J Biol Chem. 2007; 282:200–207. [PubMed: 17102138]
25. Mandella RD, Sauer LA. The mitochondrial malic enzymes. I. Submitochondrial localization and purification and properties of the NAD(P)+-dependent enzyme from adrenal cortex. J Biol Chem. 1975; 250:5877–5884. [PubMed: 238989]
26. Wise DR, Thompson CB. Glutamine addiction: a new therapeutic target in cancer. Trends Biochem Sci. 2010; 35:427–433. [PubMed: 20570523]
27. Arbiser JL, Arbiser ZK, Majzoub JA. Differential regulation of choriocarcinoma gene expression by DNA synthesis inhibitors. Endocr J. 1993; 40:263–268. [PubMed: 7951513]
28. Wise DR, DeBerardinis RJ, Mancuso A, Sayed N, Zhang XY, Pfeiffer HK, Nissim I, Daikhin E, Yudkoff M, McMahon SB, Thompson CB. Myc regulates a transcriptional program that stimulates mitochondrial glutaminolysis and leads to glutamine addiction. Proceedings of the National Academy of Sciences of the United States of America. 2008; 105:18782–18787. [PubMed: 19033189]
29. Baudino TA, McKay C, Pendeville-Samain H, Nilsson JA, Maclean KH, White EL, Davis AC, Ihle JN, Cleveland JL. c-Myc is essential for vasculogenesis and angiogenesis during development and tumor progression. Genes Dev. 2002; 16:2530–2543. [PubMed: 12368264]
30. Lauzier B, Vaillant F, Merlen C, Gelinas R, Bouchard B, Rivard ME, Labarthe F, Dolinsky VW, Dyck JR, Allen BG, et al. Metabolic effects of glutamine on the heart: Anaplerosis versus the hexosamine biosynthetic pathway. J Mol Cell Cardiol. 2013; 55:92–100. [PubMed: 23201305]
31. Wang H, Hammoudeh DI, Follis AV, Reese BE, Lazo JS, Metallo SJ, Prochownik EV. Improved low molecular weight Myc-Max inhibitors. Mol Cancer Ther. 2007; 6:2399–2408. [PubMed: 17876039]
32. Ryan J, Bloch K, Archer SL. Rodent models of pulmonary hypertension: harmonisation with the world health organisation's categorisation of human PH. International journal of clinical practice. 2011; 65(Suppl 172):15–34. [PubMed: 21736677]
33. Enns GM, Berry SA, Berry GT, Rhead WJ, Brusilow SW, Hamosh A. Survival after treatment with phenylacetate and benzoate for urea-cycle disorders. N Engl J Med. 2007; 356:2282–2292. [PubMed: 17538087]
34. Hassanein M, Hoeksema MD, Shiota M, Qian J, Harris BK, Chen H, Clark JE, Alborn WE, Eisenberg R, Massion PP. SLC1A5 mediates glutamine transport required for lung cancer cell growth and survival. Clin Cancer Res. 2013; 19:560–570. [PubMed: 23213057]

Highlights of Cardiac Glutaminolysis: A Maladaptive Cancer Metabolism Pathway in the Right Ventricule in Pulmonary Hypertension

- Patients with pulmonary artery hypertension (PAH) have evidence of cardiac glutaminolysis.
- Cardiac glutaminolysis is associated with microvascular rarefaction/ischemia.
- As in cancer, cardiac glutaminolysis results from activation of cMyc-Max.
- The specific glutaminolysis inhibitor DON regresses right ventricular hypertrophy.
- DON improves cardiac function and exercise capacity in an animal model of PAH.

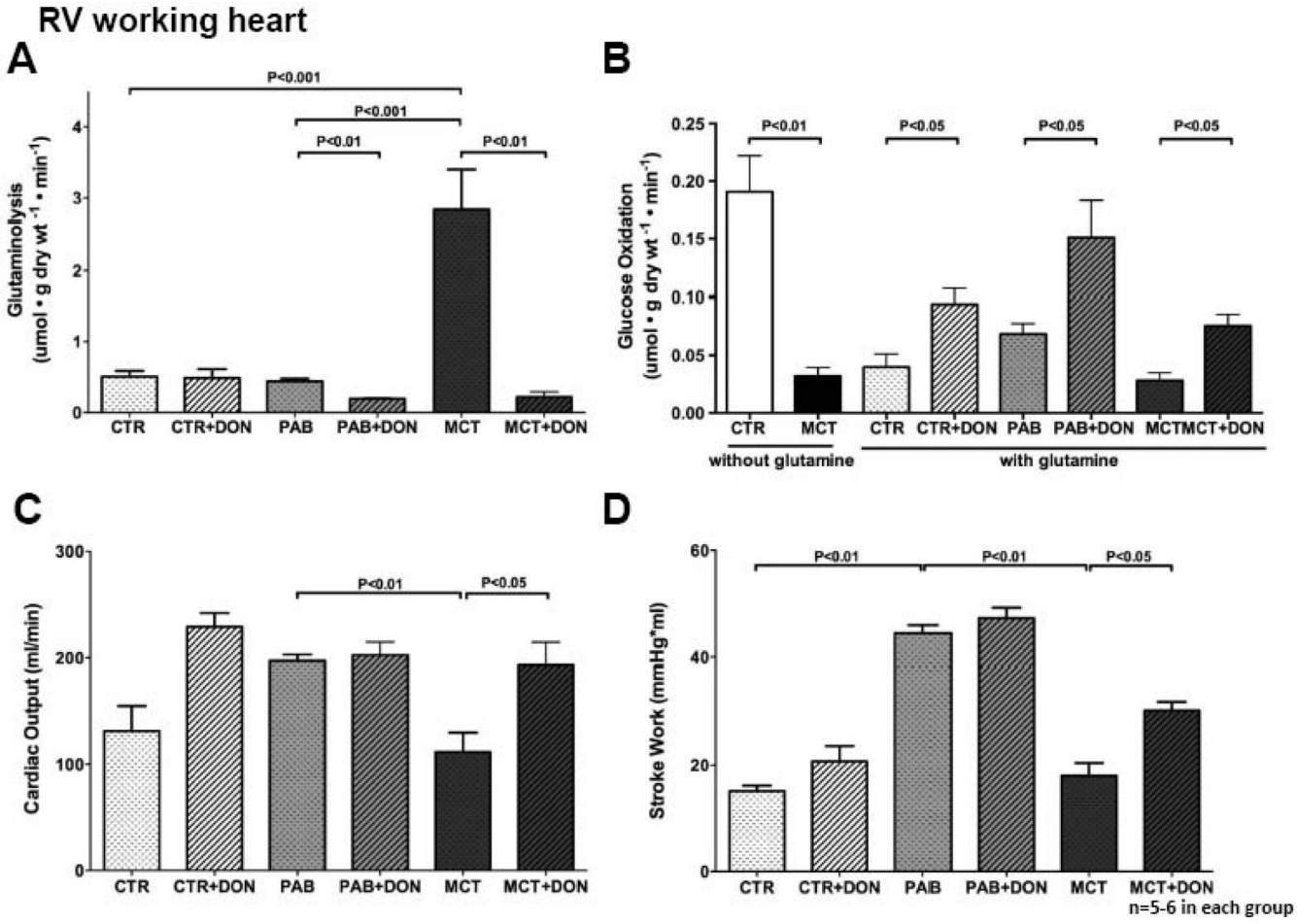

Fig 1. Glutaminolysis in RVH

A. In the RV working heart, glutaminolysis is increased in Monocrotaline-RVH, but not PAB-RVH. DON significantly reduces glutaminolysis in Monocrotaline-RVH and PAB-RVH .

B. Without glutamine (2mM) in the perfusate, glucose oxidation (GO) is decreased in Monocrotaline-RVH. In the presence of glutamine, DON increases GO in all groups.

C&D. DON improves cardiac output and stroke work in Monocrotaline-RVH.

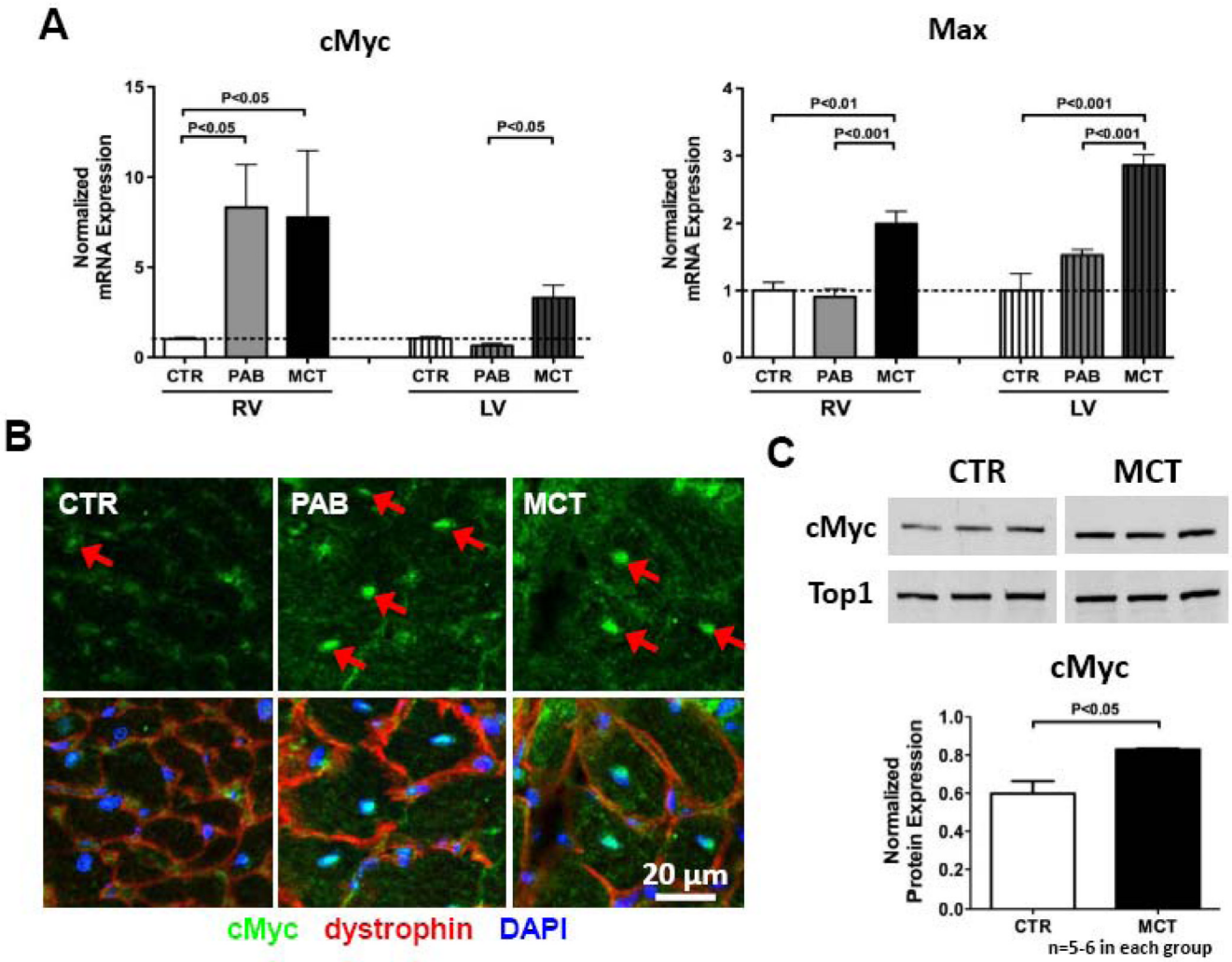

Fig 2. Increased cMyc in RVH

A. Biventricular increase in cMyc and Max mRNA in Monocrotaline-RVH. cMyc is also increased in RV in PAB-RVH. Max is not increased in PAB-RVH.

B. Representative immunostaining shows nuclear localization of cMyc in RV myocytes in RVH.

C. Immunoblot (representative gel and mean data) showing that cMyc is activated (in nuclear fractionation of cell lysates) in RVH models. Topoisomerase (Top1) is a nuclear reporter.

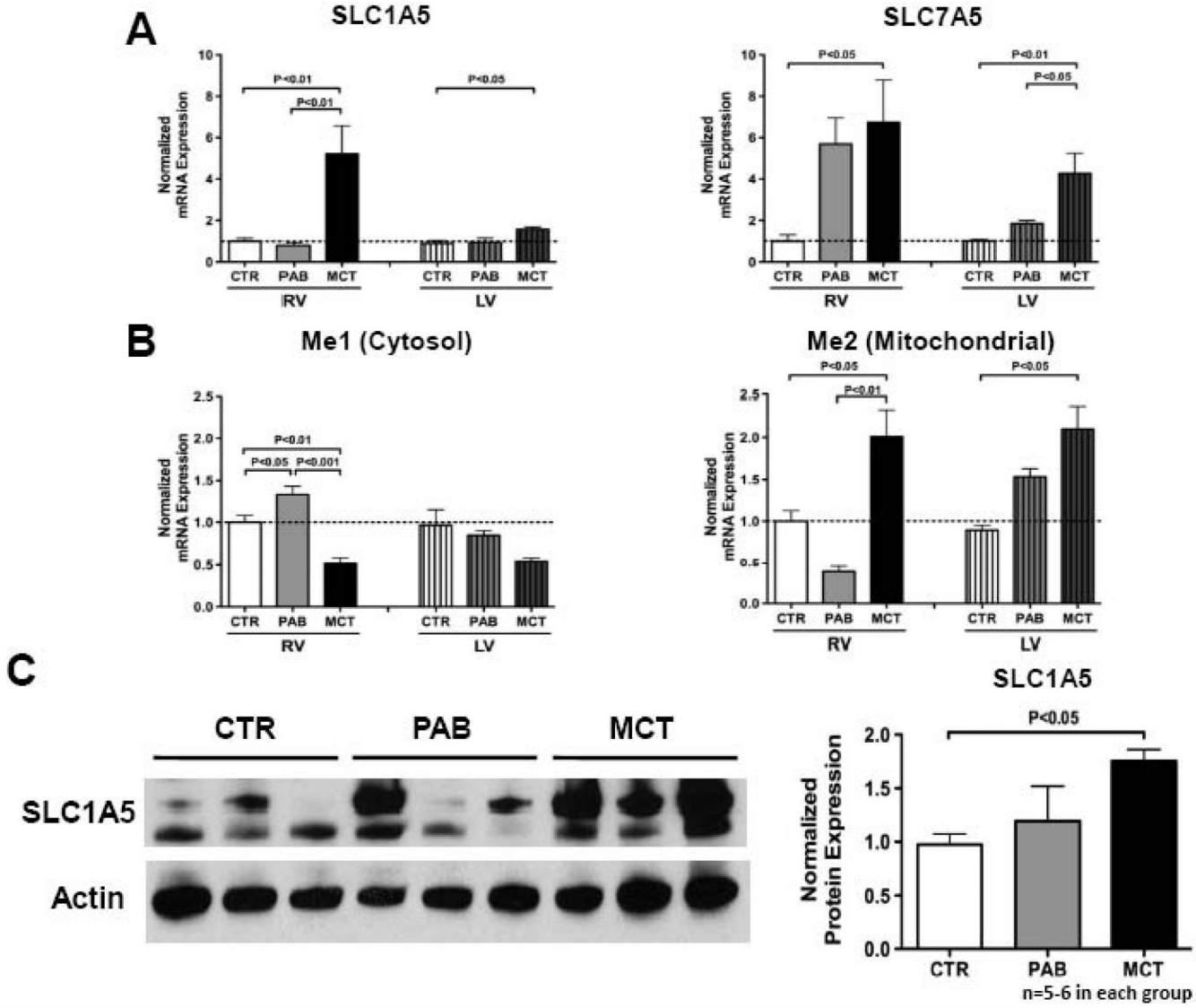

Fig 3. Upregulated Glutaminolysis in RVH

A-B. Biventricular upregulation of glutamine transporters (SLC1A5 and SLC7A5) and Me2 in Monocrotaline-RVH. In PAB-RVH, only SLC7A5 mRNA is increased in the RV.

C. Immunoblotting (representative gel and mean data) confirms the increased SLC1A5 expression in Monocrotaline- but not PAB-RVH.

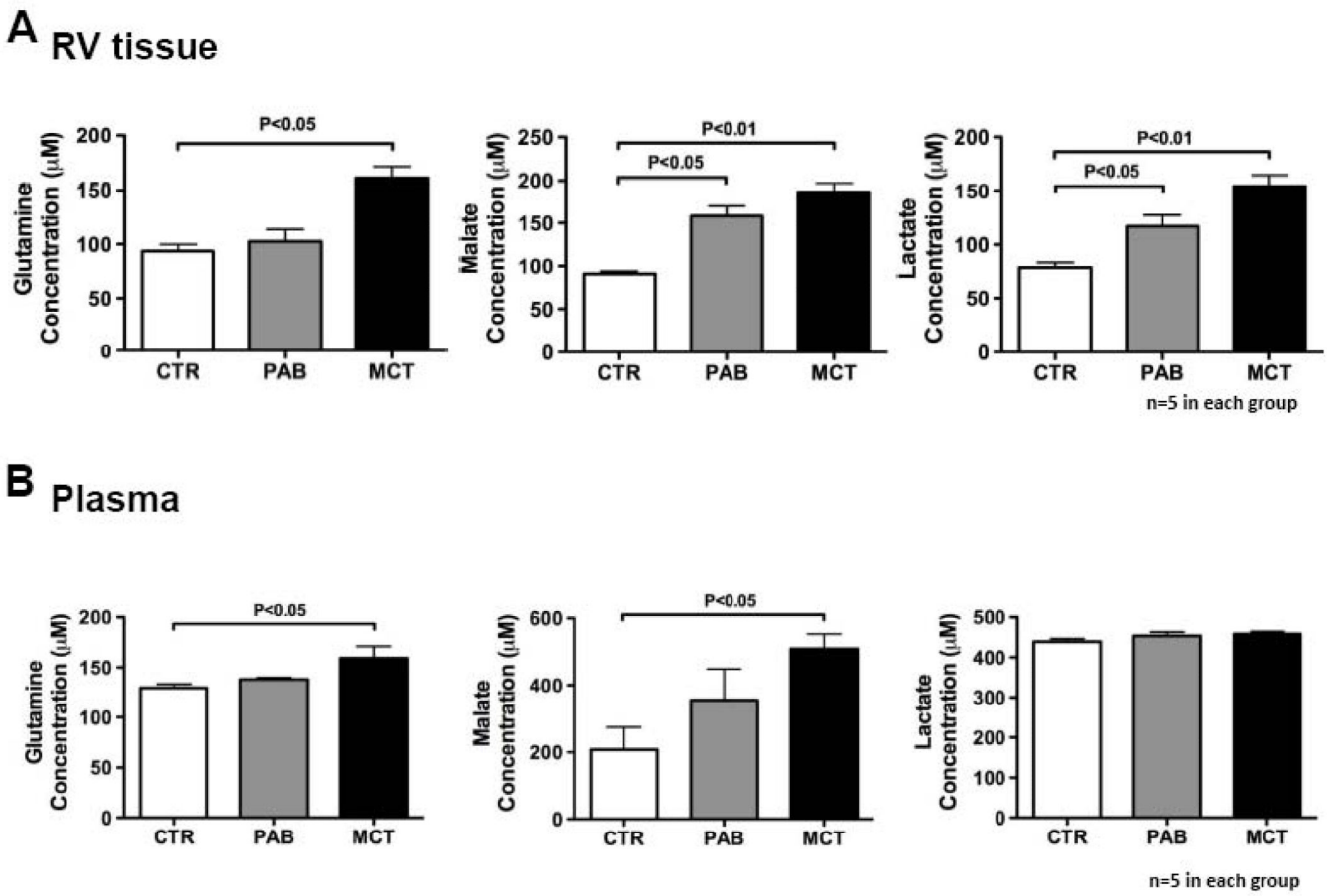

Fig 4. Glutamine, Malate and Lactate expression in RVH

A. RV cytosolic glutamine, malate and lactate are increased more in Monocrotaline-RVH than in PAB-RVH.

B. Plasma glutamine and malate are also increased more in Monocrotaline-RVH than in PAB-RVH, with no difference in plasma lactate levels.

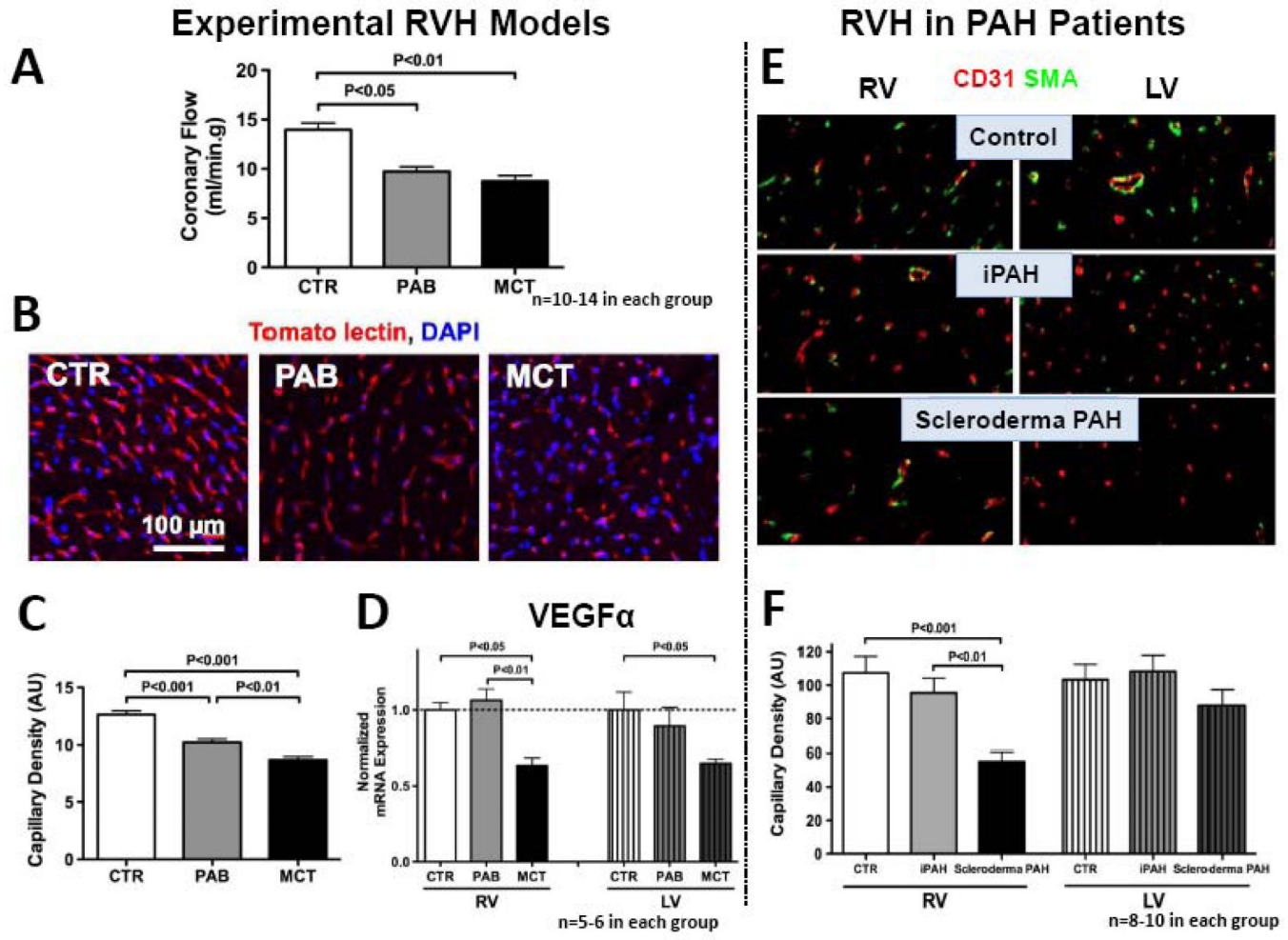

Fig 5. Ischemia and capillary rarefaction in Monocrotaline-RVH and PAH patients

A. Coronary flow in the Langendorff preparation is reduced in both RVH models.

B-C. Representative images and mean data showing greater RV capillary rarefaction in Monocrotaline-RVH, than in PAH-PVH.

D. RV VEGFα mRNA is reduced in Monocrotaline-RVH but not in PAB-RVH.

E-F. Representative images and mean data showing RV capillary rarefaction in scleroderma-PAH patients.

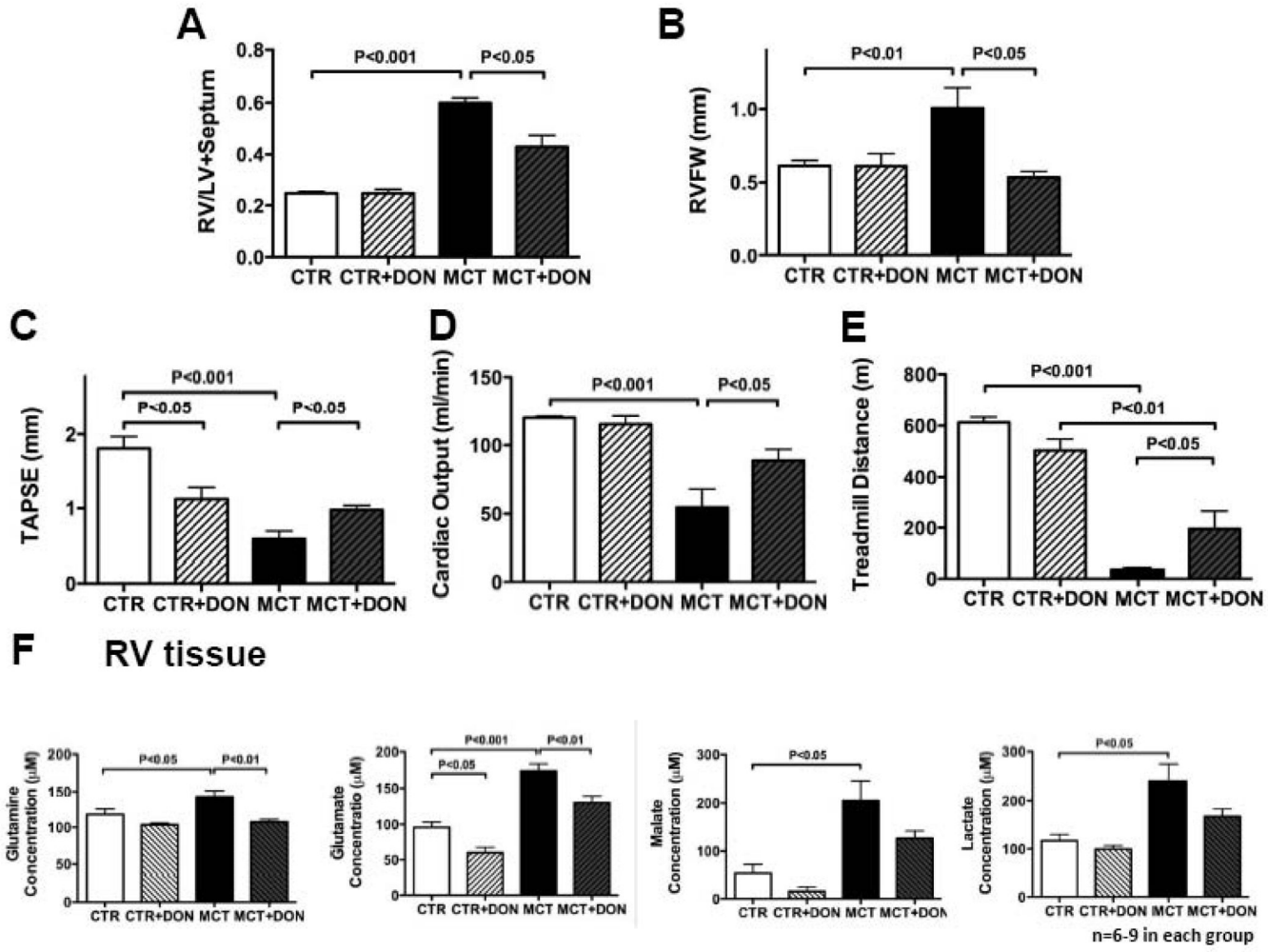

Fig 6. Chronic DON treatment improves cardiac function and treadmill capacity in Monocrotaline-RVH

A-E. DON regresses RVH and improves CO and treadmill distance in Monocrotaline-RVH.

F. DON reduces glutamine in RV myocyte cytosol and lowers mRNA expression of malate and lactate in Monocrotaline-RVH.

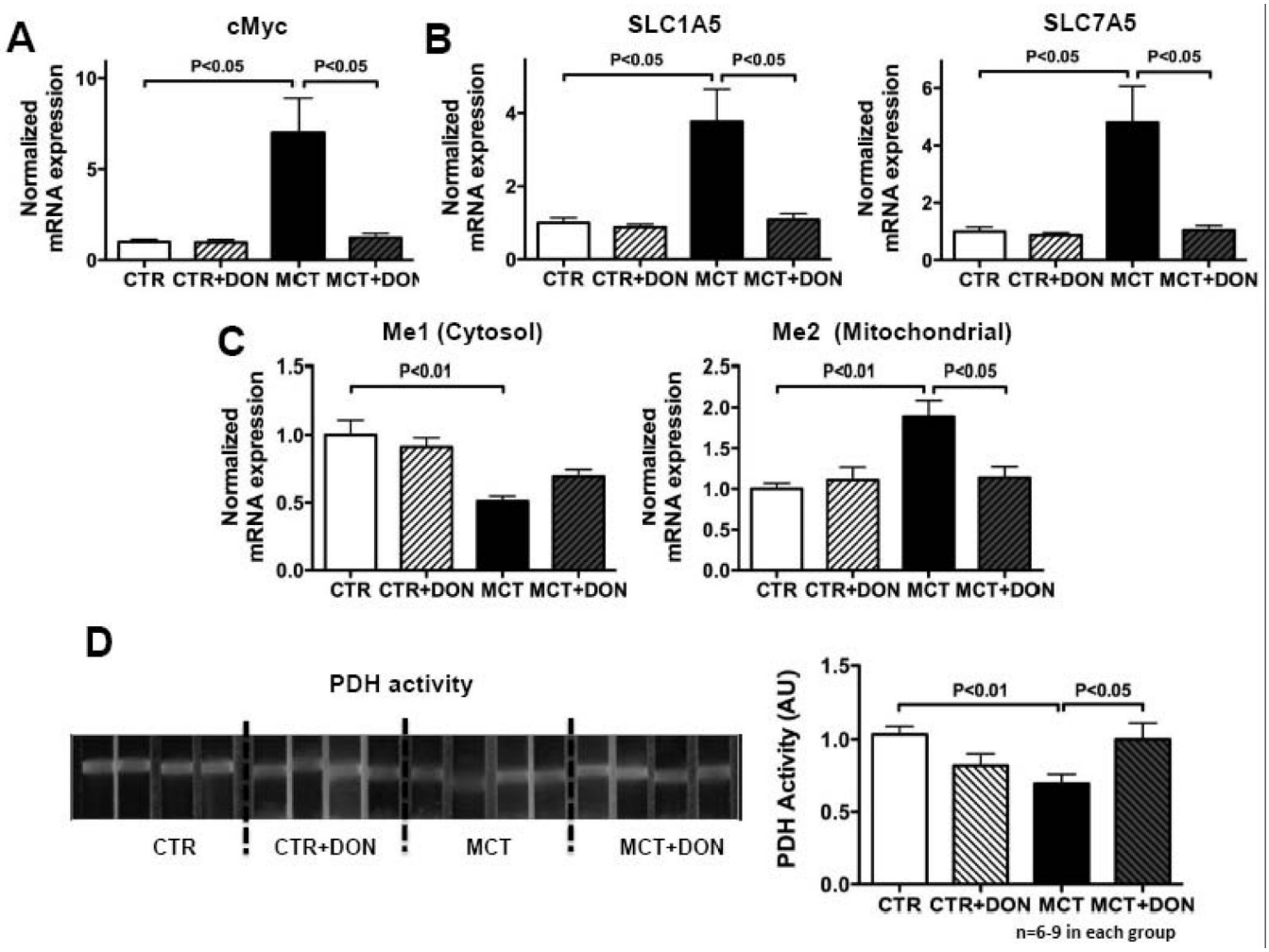

Fig 7. Chronic DON treatment decreases glutaminolysis

A-B. DON reduces cMyc, SLC1A5, SLC7A5 mRNA expression in RV myocyte cytosol in Monocrotaline-RVH.

C. Decreased cytosol Me1 expression in Monocrotaline-RV, which is slightly increased by DON. Mitochondrial Me2 mRNA expression is increased in Monocrotaline-RV and reduced by chronic DON.

D. Representative image and mean data showing that RV PDH activity is reduced in Monocrotaline-RVH and normalized by chronic DON.

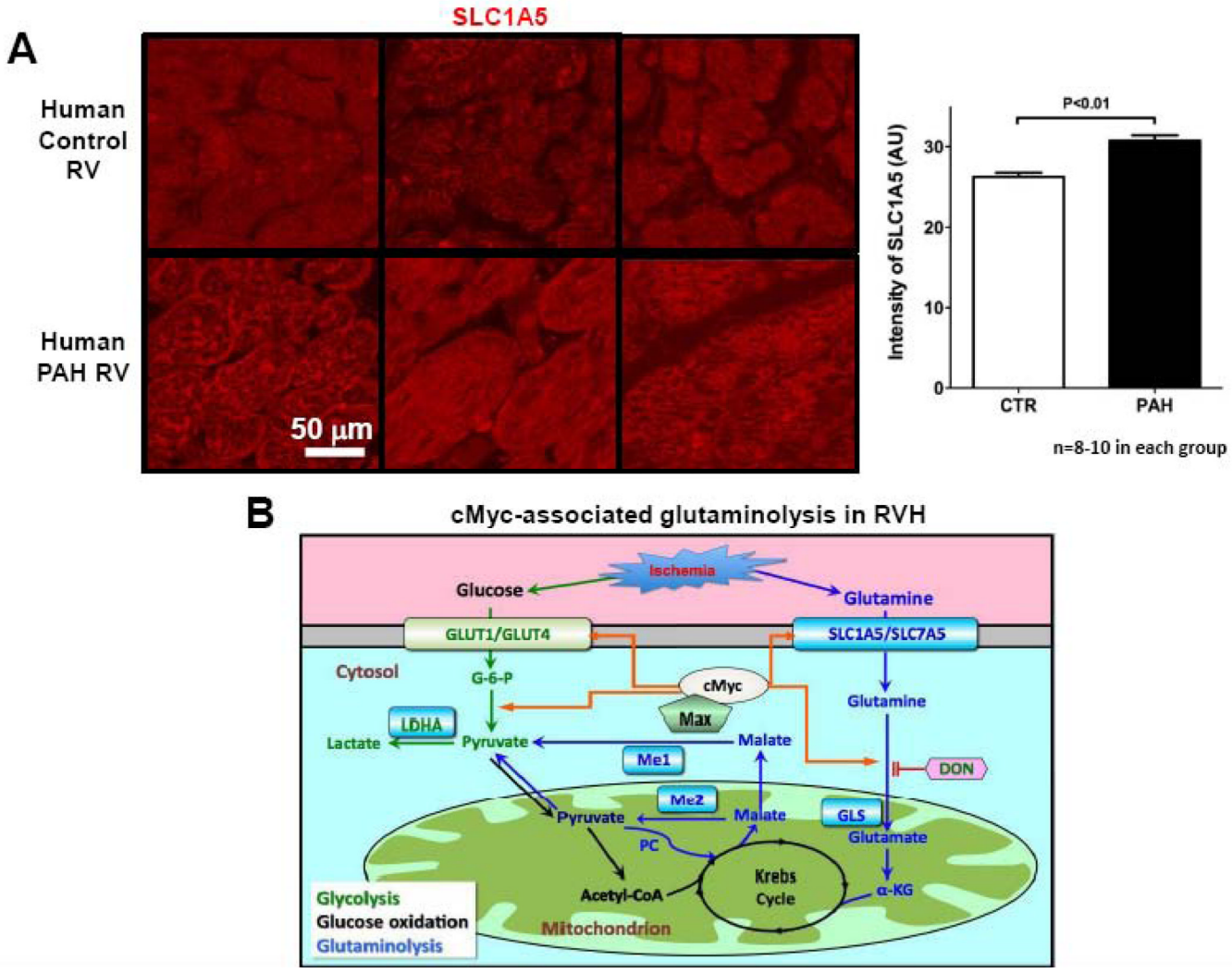

Fig 8. Mechanism for cMyc-associated glutaminolysis in RVH

A. Representative image and mean data showing increased RV myocyte plasmalemmal SLC1A5 protein in PAH patients.

B. Proposed mechanism of glutaminolysis in RVH. RV ischemia and capillary rarefaction activate cMyc and Max, which increases glutamine uptake and production of α-ketoglutarate (α-KG). α-KG enters Krebs' cycle leading to production of malate. Krebs' cycle-derived malate generates cytosolic pyruvate, which is converted by lactate dehydrogenase A (LDHA) to lactate. In conditions of high glutaminolysis GO is inhibited.